Journal of Materials Chemistry

Cite this: J. Mater. Chem., 2012, 22, 4009

www.rsc.org/materials

PAPER

Several highly efficient catalysts for Pt-free and FTO-free counter electrodes of dye-sensitized solar cells†

Yudi Wang,[a] Mingxing Wu,[a] Xiao Lin,[a] Zhicong Shi,[a] Anders Hagfeldt[b] and Tingli Ma*[a]

Received 13th October 2011, Accepted 12th December 2011
DOI: 10.1039/c2jm15182k

Three nanomaterials, namely, titanium carbide (TiC), tungsten oxide (WO_2), and vanadium nitride (VN), are introduced into dye-sensitized solar cells (DSCs) as counter electrode (CE) catalysts to replace the expensive Pt CE. Three kinds of substrates of bare glass (BG), Ti foil, and polyimide (PI) film are applied as F-doped tin oxide (FTO)-free substrates for rigid and flexible DSCs; thus realizing FTO-free and Pt-free CEs simultaneously in the DSC system. A carbon layer is used as an electron collector to replace the expensive FTO conductive layer in the insulative BG and PI film. Cyclic voltammetry, electrochemical impedance spectroscopy, and Tafel polarization curves are performed to compare the catalytic activities of these CEs for the reduction of triiodide to iodide. The results demonstrate that the DSCs that use TiC, WO_2, and VN as CEs on Ti foil have better photovoltaic performance than those that use CEs on traditional FTO glass. Moreover, the TiC, WO_2, and VN on the BG substrates show excellent catalytic activities that can match the performance of the CEs on FTO glasses.

Introduction

In 1991, Grätzel *et al.* reported a novel dye-sensitized solar cell (DSC) that rapidly gained attention because of its high efficiency, low cost, environmental friendliness, and simple fabrication.[1,2] Typically, a DSC consists of a dye-sensitized nanocrystalline TiO_2 semiconductor electrode, a counter electrode (CE), and an electrolyte containing a triiodide/iodide redox couple.

Generally, the CE of a DSC applies an F-doped tin oxide (FTO) glass coated with a Pt film. Pt acts as a catalyst to reduce triiodide to iodide in the electrolyte. However, although Pt has good catalytic activity, it is an expensive noble metal. Recently, many researchers have focused on exploiting inexpensive substitutes for Pt, such as carbon materials,[3–9] conductive organic polymers,[10–12] and inorganic materials.[13–16]

FTO glass is used as conductive substrate. Unfortunately, it accounts for approximately 60% of the total cost of DSCs. The FTO layer is essential for the high conductivity and transparency of CEs, but its high cost limits the mass production of DSCs that make use of FTO glass.[17–19] Moreover, the FTO glass has shape limitations and is fragile, thus restricting the applications of DSCs in many fields. Therefore, developing new non-Pt catalysts and FTO-free substrates to reduce the cost of DSCs and to enhance the competitiveness of this system among various photovoltaic devices is necessary.

In recent studies, flexible graphite sheets coated with active carbon,[20] submicrometer-sized graphite,[19] conductive poly(3,4-alkylenedioxythiophene) film,[17] and polyaniline nanofiber deposited on carbon films[21] have been used as Pt-free or FTO-free CEs in flexible DSCs. However, they have shown low conversion efficiencies because of their low catalytic activities. To date, no study on transition metal compounds acting as high-performance catalysts deposited on non-FTO substrates has been published.

Three kinds of substrates and three catalytic materials as CEs in DSC systems were developed in the present study. Their performances were compared with that of traditional Pt CE deposited on FTO glass under the same conditions. The substrates included bare glass (BG) for rigid substrate, and titanium foil (Ti) and polyimide film (PI) for flexible substrates. The catalytic materials included titanium carbide (TiC), tungsten oxide (WO_2), and vanadium nitride (VN). The energy conversion efficiencies of the DSCs based on the three catalysts and three kinds of substrates were investigated. The results showed that the performance of the DSCs based on TiC CE coated on BG, Ti, and PI substrates were 5.71%, 7.15%, and 3.90%, respectively. WO_2 and VN also showed high catalytic activities on various FTO-free substrates.

Experimental

Preparation of photoanode

A semi-conductive TiO_2 (Degussa, Germany) film with 12 μm thickness on an ultrasonically cleaned FTO glass was fabricated

[a]State Key Laboratory of Chemicals, School of Chemial Engineering, Dalian University of Technology, Dalian, China. E-mail: tinglima@dlut.edu.cn; Fax: +86-411-84986230; Tel: +86-411-84986237
[b]Department of Physical and Analytical Chemistry, Uppsala University, Box 259, SE-751 05 Uppsala, Sweden

† Electronic supplementary information (ESI) available. See DOI: 10.1039/c2jm15182k

using a screen-printing technique. The TiO_2 film was sintered at 500 °C for 30 min, and then subsequently cooled to 80 °C. Finally, the TiO_2 film was immersed in a 5×10^{-4} M solution of N719 dye (Solaronix SA, Switzerland) in acetonitrile/*tert*-butanol (volume ratio 1 : 1) for 22 h to obtain the photoanode.

Preparation of CE

WO_2 and VN were synthesized using a simple chemical method according to previous reports.[22,23] TiC was obtained commercially. Up to 500 mg TiC was dispersed with 10 mL isopropanol in an agate pot, and was milled for 4 h using a star ball mill (QM-QX04, Nanjing NanDa Instrument Plant), resulting in a TiC slurry. The preparation of WO_2 and VN slurries were similar to that of the TiC slurry. The electrodes of the three kinds of catalytic materials were similarly manufactured. For the TiC electrodes, the prepared TiC slurry was sprayed on an FTO glass (Asahi Glass, Type-U, 25 Ω sq^{-1}; Japan) using an airbrush connected to a mini compressor, and then sintered in a N_2 atmosphere at 400 °C for 30 min in a tube furnace to prepare the FTO/TiC CE. A conductive carbon (CC, Shenzhen DongDaLai Chemical Co., Ltd.) layer was coated on the BG substrate using the doctor-blading technique. The BG substrate was then annealed at 150 °C for 30 min. The TiC slurry was sprayed on the surface and sintered in a N_2 atmosphere at 400 °C for 30 min to prepare the BG/CC/TiC CE. The SEM image of the BG/CC/TiC CE is shown in Fig. S1 to determine the thickness of CC layer.† For the Ti foil (0.2 mm, Baoji Deli Titanium Industry Co.) substrate, pretreatment of Ti foil was performed by immersing it in a mixture of hydrofluoric acid and deionized water (v : v = 1 : 3) and a mixture of concentrated nitric acid and deionized water (v : v = 1 : 6) alternately at 1 min each. The Ti foil was then ultrasonically cleaned in ethanol. Subsequently, the TiC slurry was sprayed on the Ti foil and sintered in a N_2 atmosphere at 400 °C for 30 min in a tube furnace. A CC layer was coated on the PI film (0.1 mm, MGC, Inc. Japan) substrate using the doctor-blading technique. The PI film was then annealed at 150 °C for 30 min to obtain the PI/CC. The TiC slurry was sprayed on the surface of the PI/CC and sintered in a N_2 atmosphere at 250 °C for 30 min to prepare the PI/CC/TiC CE. Based on the procedures mentioned above, the WO_2 and VN electrodes on various substrates can be prepared easily. The FTO/Pt electrode was prepared based on our previous research.[24–26] The BG/CC/Pt CE was prepared as follows: a CC layer was coated on the BG using the doctor-blading technique. The BG was then annealed at 150 °C for 30 min. H_2PtCl_6 solution was sprayed on the BG, which was then sintered in a N_2 atmosphere at 400 °C for 30 min.

Characterization

The four-point probe method (RTS-9, Four Probes Tech, Guangzhou) was used to measure the sheet resistances of the CEs. The thickness of CC/TiC CE on bare glass was characterized by scanning electron microscopy (SEM) using FEI Hitachi S-4800 and KYKY2800. The DSCs with active areas of 0.16 cm^2 used for the photovoltaic performance tests were fabricated using a photoanode, a CE, and an electrolyte containing 1 M 1-propyl-3-methylimidazolium iodide, 0.15 M I_2, 0.5 M 4-*tert*-butyl pyridine, and 0.1 M guanidinium thiocyanate in Γ-butyrolactone. The current–voltage (*I–V*) characteristics of the DSCs were measured in simulated AM 1.5 illumination (100 mW cm^{-2}; Peccell-L15, Peccell, Japan) using a Keithley digital source meter (Keithley 2601, USA).

The symmetrical dummy cell was assembled by stacking two identical electrodes facing each other and filling the electrolyte similar to that described above, which was used in the electrochemical impedance spectroscopy (EIS) experiments and Tafel-polarization tests. The EIS measurements were conducted in the dark at room temperature using a computer-controlled potentiostat (Zennium Zahner, Germany), with a frequency range of 100 mHz–1 MHz, AC amplitude of 10 mV, and bias of −0.75 V. The spectra were then fitted using Zview software. The Tafel-polarization curves were measured using an electrochemical work station system (LK-9805, Tian Jin Lanli Inc.) at a scan rate of 10 mV s^{-1}. Cyclic voltammetry (CV) was performed in a three-electrode system in an acetonitrile solution containing 0.1 M $LiClO_4$, 10 mM LiI, and 1 mM I_2 at a scan rate of 10 mV s^{-1}, with a CE of Pt and an Ag/Ag^+ reference electrode.

Results and discussion

An electron-collecting layer with good adhesion and conductivity in FTO-free CE is essential for efficient charge transport. CC may replace the FTO glass because of its excellent electrical conductivity (EC), low sheet resistance of 10 Ω sq^{-1}, and good adhesion. Pt-based CEs were prepared on FTO glass (FTO/Pt) and CC coated BG (BG/CC/Pt) under similar conditions to investigate the effect of CC when deposited on BG substrates as an electron collector compared with traditional FTO glass. The sheet resistances of the two CEs were 6.7 Ω sq^{-1} for FTO/Pt and 4.7 Ω sq^{-1} for BG/CC/Pt, ascribed to the low sheet resistance of CC compared with that of FTO glass. CV was conducted to assess the electrochemical catalytic activities for triiodide reduction. Fig. 1 shows the CVs of the FTO/Pt and BG/CC/Pt *versus* the Ag/Ag^+ reference electrode. Two pairs of nearly reversible redox peaks were observed for both FTO/Pt and BG/CC/Pt electrodes. Based on previous studies,[27] the relatively negative pair of redox peaks can be assigned to the redox reaction given by

$$I_3^- + 2e^- \rightleftharpoons 3I^- \quad (1)$$

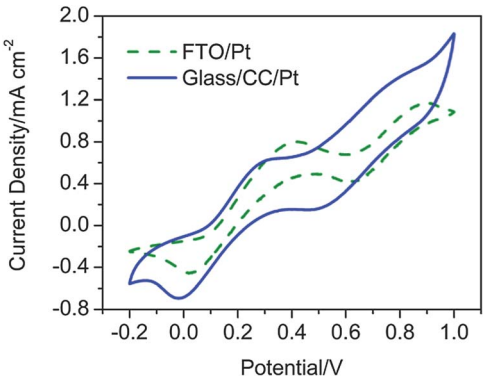

Fig. 1 CVs of the FTO/Pt and BG/ CC/Pt electrodes for triiodide/iodide redox couple.

The relatively positive pair can be assigned to the reaction given by

$$3I_2 + 2e^- \rightleftharpoons 2I_3^- \quad (2)$$

The current densities of the two CEs were similar, indicating similar electrocatalytic behavior. Thus, CC is as effective as FTO at being an electron collector.

Fig. 2 shows the photocurrent density–photovoltage (*I–V*) characteristics of the DSCs fabricated with FTO/Pt and BG/CC/Pt CEs. The photovoltaic parameters are listed in Table 1. The DSC with BG/CC/Pt CE achieved a power conversion efficiency of 6.64%, which was 96.9% of that using FTO/Pt CE. The two CEs displayed similar open circuit voltage (V_{oc}) values with variations in short circuit current density (J_{sc}) and fill factor (*FF*). The high *FF* of BG/CC/Pt CE may be attributed to the low sheet resistance of CC.

EIS was performed on the symmetrical dummy cells to evaluate the electrochemical characteristics of the two CEs. Fig. 3(a) shows the Nyquist plots. The high frequency intercept on the real axis corresponds to the series resistance (R_s). The first semicircle at the high-frequency region arises from the charge transfer property (R_{ct}) and the corresponding capacitance at the electrode/electrolyte interface, whereas the other semicircle at the low-frequency region arises from the Nernst diffusion impedance (Z_N) of the triiodide/iodide in the electrolyte. The corresponding parameters were obtained by fitting the impedance plots using Zview software based on an equivalent circuit model, as shown in Fig. 3(b). The calculated R_{ct} of the BG/CC/Pt was close to that of FTO/Pt, whereas the R_s of the two dummy cells were diverse, as shown in Table 1. The BG/CC/Pt CE had slightly larger R_s than the FTO/Pt CE, indicating that CC was an effective electron collector. The R_{ct} of both BG/CC/Pt and FTO/Pt were less than 10 Ω; thus demonstrating that they were effective in catalyzing triiodide reduction. This finding is in good agreement with the photovoltaic performances of the DSCs using the two CEs.

As shown in Fig. 4, Tafel polarization curve, a powerful electrochemical characterization measurement, was performed on the dummy cells to confirm the catalytic activities of the two CEs. Theoretically, the Tafel curve can be divided into three zones. The curve at the very high potential corresponds to the limiting diffusion zone, which depends on the transport of triiodide and iodide in the electrolyte. The curve at the relatively low potential but higher than 120 mV corresponds to the Tafel zone, where voltage (*E*), a linear function of the logarithm of the current density (lg*I*), is given by

$$E = \frac{2.3RT(\lg I - \lg I^0)}{\alpha nF} \quad (3)$$

where *R* is the gas constant, *T* is the temperature, α is the distribution coefficient, *F* is Faraday's constant, and *n* is the number of electrons involved in the reaction at the electrode.

Based on eqn (3), the information on the exchange current density (I^0) at this region can be obtained by extending the line to the voltage as zero, and then receiving the current density (*I*) thereafter. Thus, a steep slope of the Tafel zone holds a large I^0 to some extent. The curve at the very low potential, also known as the polarization zone, arises from the electrochemical reaction, where *E* is a linear function of *I*. The slope of this region can represent R_{ct} as follows:

$$R_{ct} = \frac{RT}{nFI^0} \quad (4)$$

where *R* is the gas constant, *T* is the temperature, *F* is Faraday's constant, and *n* is the number of electrons involved in the reaction at the electrode.

From Fig. 4, BG/CC/Pt CE demonstrates a slightly gentler slope than the FTO/Pt CE, indicating a smaller I^0 and a relatively lower catalytic activity, in agreement with the EIS results and the photovoltaic performances of the DSCs.

The results showed that CC is an excellent substitute for FTO as an electron collector in DSC systems. The three highly efficient catalytic materials, namely, TiC, WO_2, and VN, were applied in DSCs to replace the expensive Pt as CEs. Ti foil and PI film were included among the non-FTO substrates for flexible CEs. Ti foil with 0.2 mm thickness possesses good flexibility and remarkable EC, while the PI film has the advantages of thermostability up to 300 °C, transparency and low cost over the conventional indium tin oxide-polyethylene naphthalate flexible substrate.

The three non-Pt catalytic materials were deposited on the three FTO-free substrates BG, Ti, and PI as CEs to assemble low-cost DSCs. TiC, WO_2, and VN were deposited on the FTO glasses for comparative research. Fig. 5 shows the *I–V* curves of the DSCs mentioned above. Table 2 shows their corresponding photovoltaic parameters. For the FTO glass, the energy conversion efficiencies of TiC, WO_2, and VN were 6.29%, 6.00%, and 6.29%, respectively (the Nyquist plots and EIS parameters of the dummy cells using TiC, WO_2, and VN electrodes deposited on FTO substrate are available in the ESI†). The photovoltaic performances of the three low-cost materials showed that they were highly effective in catalyzing the reduction of triiodide to iodide. For the rigid BG, the energy conversion efficiencies decreased to 80%–90% of those on the FTO glass due to the decrease in *FF*. For the Ti foil substrate, the DSCs fabricated with TiC, WO_2, and VN CEs demonstrated much higher efficiencies of 7.15%, 7.13%, and 6.97%, respectively, than those fabricated on FTO glasses. For the PI film substrate, the efficiencies were comparatively low because of the relatively low J_{sc} and *FF* due to the large R_s.

A number of electrochemical experiments were conducted to further investigate the effects of the substrates on the

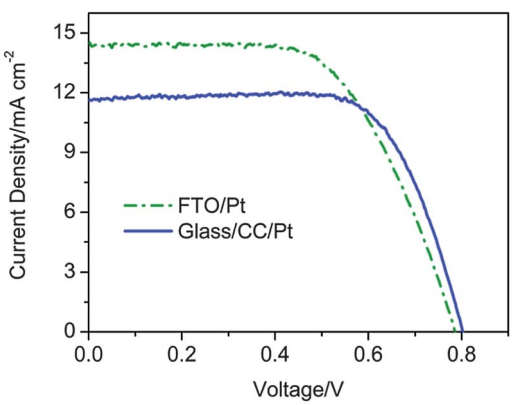

Fig. 2 Photocurrent density–photovoltage (*I–V*) curves of the DSCs that use FTO/Pt and BG/CC/Pt as CEs.

Table 1 Photovoltaic parameters of the DSCs using FTO/Pt and BG/CC/Pt CEs and EIS parameters of the dummy cells based on two identical electrodes

CE	Sheet resistance/Ω sq^{-1})	V_{oc}/V	J_{sc}/mA cm^{-2}	*FF*	η (%)	R_s/Ω	R_{ct}/Ω	Z_N/Ω
FTO/Pt	6.7	0.79	14.44	0.60	6.85	30.58	6.42	111.6
BG/CC/Pt	4.7	0.80	11.64	0.71	6.64	52.23	8.65	103.8

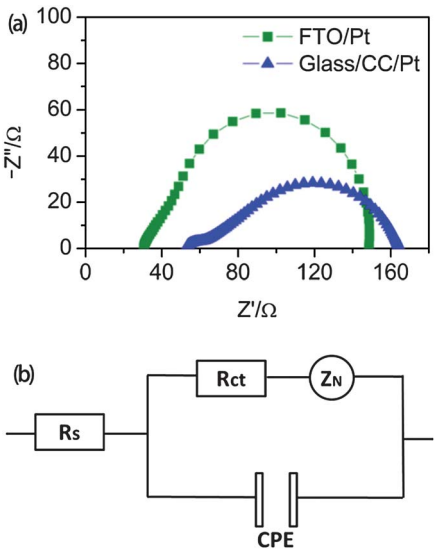

Fig. 3 (a) Nyquist plots of the dummy cells based on the FTO/Pt and BG/CC/Pt electrodes; (b) equivalent circuit diagram.

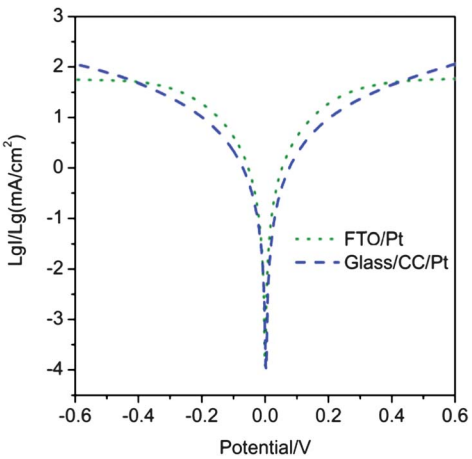

Fig. 4 Tafel curves of the dummy cells fabricated with FTO/Pt and BG/CC/Pt electrodes.

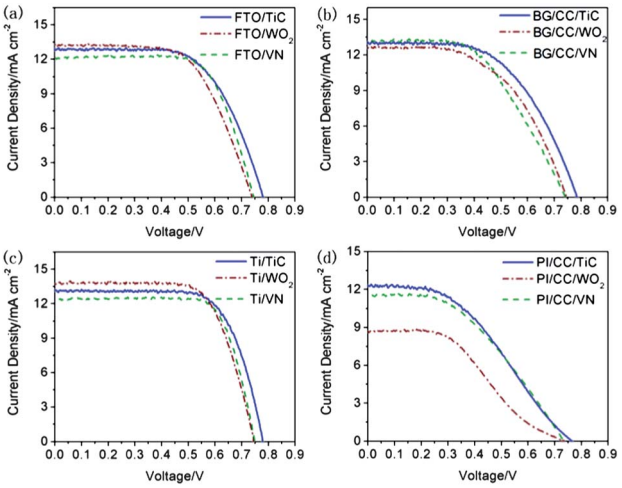

Fig. 5 *I–V* curves of the DSCs using TiC, WO_2, and VN as CEs deposited on the four substrates: (a) FTO; (b) BG; (c) Ti; (d) PI.

Table 2 Photovoltaic parameters of the DSCs using TiC, WO_2, and VN deposited on four substrates as CEs

CEs	V_{oc}/V	J_{sc}/mA cm^{-2}	*FF*	η (%)
FTO/TiC	0.78	12.91	0.62	6.29
FTO/WO_2	0.74	13.24	0.61	6.00
FTO/VN	0.75	12.14	0.69	6.29
BG/CC/TiC	0.79	12.98	0.56	5.71
BG/CC/WO_2	0.75	12.59	0.54	5.09
BG/CC/VN	0.74	13.19	0.52	5.13
Ti/TiC	0.78	13.12	0.70	7.15
Ti/WO_2	0.75	13.78	0.69	7.13
Ti/VN	0.75	12.42	0.75	6.97
PI/CC/TiC	0.77	12.32	0.41	3.90
PI/CC/WO_2	0.74	8.74	0.40	2.60
PI/CC/VN	0.73	11.46	0.44	3.72
Pt	0.77	14.49	0.65	7.35

performances of the CEs, with TiC as a typical example. Fig. 6 shows the CVs of the triiodide/iodide redox for the four TiC-coated substrates of FTO, BG, Ti, and PI. Two typical pairs of oxidation and reduction peaks were obtained for the FTO/TiC, BG/CC/TiC, and Ti/TiC electrodes. The cathodic peaks of these CEs, with values of approximately 0.05 and 0.54 V, can be assigned to the reactions of eqn (1) and (2). The PI/CC/TiC CE exhibited a pair of redox peaks assigned to the reaction of eqn (1). The potential separation between the oxidation and reduction peaks was much larger than that of the other three CEs, indicating a poorer reversibility of PI/CC/TiC CE in catalyzing the reduction of triiodide to iodide. These findings conform to the *I–V* results, as shown in Fig. 7. The photovoltaic parameters are collated in Table 3. The DSC using Ti/TiC CE achieved the highest energy conversion efficiency of 7.15% among the four CEs, with a large J_{sc} of 13.12 mA cm^{-2} and a high *FF* of 0.7. The V_{oc} and J_{sc} of Ti/TiC were similar to those of the FTO/TiC and BG/CC/TiC CEs. The *FF* differences between Ti/TiC, FTO/TiC, and BG/CC/TiC lead to their different efficiencies. The highest FF of Ti/TiC can be attributed to the high EC of the Ti sheet. The decreased efficiency of the PI/CC/TiC CE was

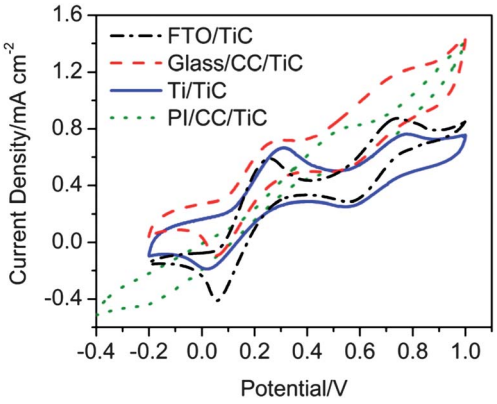

Fig. 6 CV curves of the triiodide/iodide redox couple for the four kinds of TiC electrodes.

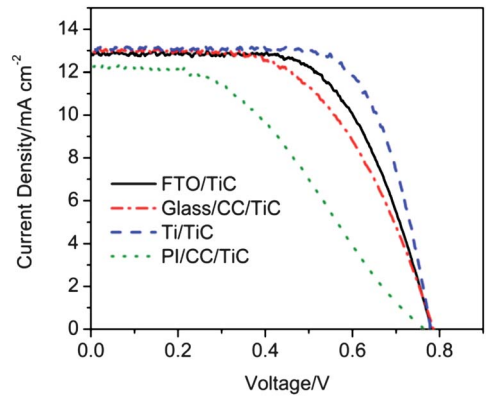

Fig. 7 Photocurrent–voltage (*I*–*V*) curves of the DSCs using TiC-coated FTO, BG, Ti, and PI as CEs.

due to J_{sc} and *FF*. Table 3 shows the sheet resistances of the four CEs measured using the four-point probe method. The values are 6.63, 4.64, 0.0094, and 16.86 Ω sq^{-1} for FTO/TiC, BG/CC/TiC, Ti/TiC, and PI/CC/TiC, respectively.

The catalytic activity that stemmed from R_{ct} in the electrode/electrolyte interface and R_s affects the photovoltaic performances of J_{sc} and *FF*. Thus, EIS measurements were conducted in the dummy cells to evaluate the differences in the R_{ct} and R_s of the CEs using the four substrates. Fig. 8 shows the Nyquist plots of the dummy cells. The EIS parameters shown in Table 3 were calculated by fitting the plots. The Z_N of the four CEs were approximately 100 Ω. The Ti/TiC electrode had the smallest R_s of 1.83 Ω and R_{ct} of 0.28 Ω, derived from the excellent electrical conductivity of the Ti foil, the firm bonding strength between the TiC and Ti foil, and the high catalytic activity of TiC. The excellent performance of the Ti/TiC CE generated the highest energy conversion efficiency of 7.15%. The R_s (28.4 Ω) and R_{ct} (6.5 Ω) of the BG/CC/TiC electrode were a little larger than those of the FTO/TiC electrode (R_s = 18.8 Ω, R_{ct} = 4.3 Ω), indicating that the less-firm bonding strength between TiC and CC leads to the decrease in the *FF* of BG/CC/TiC CE. However, J_{sc} not only depends on the bonding strength between the TiC and the substrate in charge of R_s and R_{ct}, but also on the EC of the CE in charge of the sheet resistance. Although the R_s and R_{ct} of BG/CC/TiC were larger than those of FTO/TiC, the sheet resistance of BG/CC/TiC was smaller. They counterbalanced each other, thus resulting in a homologous J_{sc} for the BG/CC/TiC and FTO/TiC CEs. For the PI/CC/TiC electrode, the R_s, R_{ct}, and sheet resistance were all large, which might be ascribed to the weak bonding force between the CC and PI film due to the low sintering temperature of 250 °C, and the reduced EC of the CC layer, resulting in poor *FF* and J_{sc}.

Tafel polarization curves were generated to verify the electrochemical catalytic activities of the four CEs. Fig. 9 shows the Tafel curves with lg*I* as a function of *E*. From the Tafel zone, the Ti/TiC electrode displayed the largest I^0, followed by the FTO/

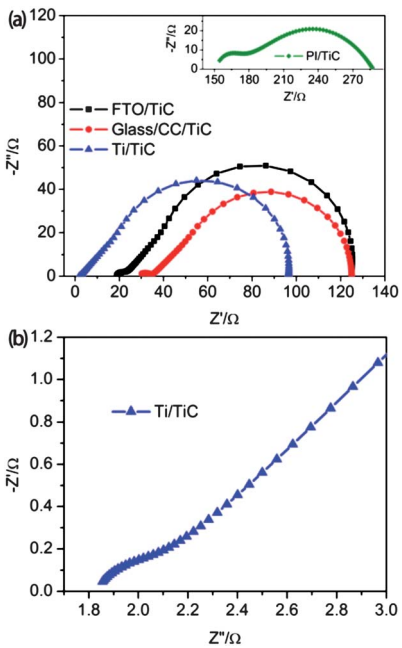

Fig. 8 (a) Nyquist plots of the dummy cells based on four kinds of TiC electrodes; (b) enlarged view of Nyquist plot of the dummy cell based on Ti/TiC electrode.

Table 3 Photovoltaic parameters of the DSCs using TiC deposited onto four kinds of substrates as CEs and EIS parameters of the dummy cells based on these electrodes

CEs	Sheet resistance/Ω sq^{-1})	V_{oc}/V	J_{sc}/mA cm^{-2}	*FF*	η (%)	R_s/Ω	R_{ct}/Ω	Z_N/Ω
FTO/TiC	6.63	0.78	12.91	0.62	6.29	18.84	4.30	101.6
BG/CC/TiC	4.64	0.79	12.98	0.56	5.71	28.40	6.50	90.1
Ti/TiC	0.0094	0.78	13.12	0.70	7.15	1.83	0.28	94.3
PI/CC/TiC	16.86	0.77	12.32	0.41	3.90	151.2	15.53	120.7

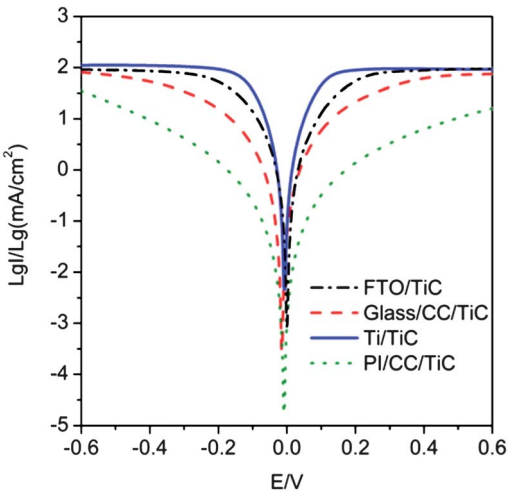

Fig. 9 Tafel curves of the TiC electrode loaded on various electrodes.

TiC and BG/CC/TiC electrodes. The PI/CC/TiC electrode presented the smallest I^0. These findings show that similar R_{ct} trends can be obtained from EIS according to eqn (4). The results were in good agreement with the photovoltaic performance.

Conclusions

A series of low-cost counter electrodes without expensive Pt catalyst and FTO layer were developed in the current study. Highly efficient catalysts, namely TiC, WO_2, and VN, were proposed to replace the expensive Pt. All the catalysts performed well. The high-performance catalysts were deposited on three kinds of low-cost substrates to replace the FTO glass, including rigid BG, Ti foil, and PI film for flexible DSCs. For the insulative materials of BG and PI film, the CC layers deposited on these substrates acted as electron collectors. The DSCs that use CEs on the Ti substrate showed the best photovoltaic performance, exceeding that of the CEs on traditional FTO glass. The DSCs with CEs on the BG substrate also exhibited relatively high efficiencies that can match the performances of the CEs on FTO glass. The present study provided a series of low-cost and highly efficient CEs for DSCs.

Acknowledgements

This research was supported by the National Natural Science Foundation of China (Grant No. 50773008). It was also supported by the National High Technology Research and Development Program for Advanced Materials of China (Grant No. 2009AA03Z220).

Notes and references

1 B. O'Regan and M. Grätzel, *Nature*, 1991, **353**, 737.
2 M. Grätzel, *Nature*, 2001, **414**, 338.
3 E. Ramasamy, W. J. Lee, D. Y. Lee and J. S. Song, *Appl. Phys. Lett.*, 2007, **90**, 173103.
4 E. Ramasamy, W. J. Lee, D. Y. Lee and J. S. Song, *Electrochem. Commun.*, 2008, **10**, 1087.
5 G. Q. Wang, W. Xing and S. P. Zhuo, *J. Power Sources*, 2009, **194**, 568.
6 P. Joshi, Y. Xie, M. Ropp, D. Galipeau, S. Bailey and Q. Q. Qiao, *Energy Environ. Sci.*, 2009, **2**, 426.
7 W. J. Hong, Y. X. Xu, G. W. Lu, C. Li and G. Q. Shi, *Electrochem. Commun.*, 2008, **10**, 1555.
8 M. X. Wu, X. Lin, T. H. Wang, J. S. Qiu and T. L. Ma, *Energy Environ. Sci.*, 2011, **4**, 2308.
9 S. I. Cha, B. K. Koo, S. H. Seo and D. Y. Lee, *J. Mater. Chem.*, 2010, **20**, 659.
10 Q. H. Li, J. H. Wu, Q. W. Tang, Z. Lan, Q. J. Li, J. M. Lin and L. Q. Fan, *Electrochem. Commun.*, 2008, **10**, 1299.
11 K.-M. Lee, C.-Y. Hsu, P.-Y. Chen, M. Ikegami, T. Miyasaka and K.-C. Ho, *Phys. Chem. Chem. Phys.*, 2009, **11**, 3375.
12 H. Q. Jiang, S. Sakurai and K. Kobayashi, *Electrochem. Solid-State Lett.*, 2009, **12**, F13.
13 M. K. Wang, A. M. Anghel, B. Marsan, N. C. Ha, N. Pootrakulchote, S. M. Zakeeruddin and M. Grätzel, *J. Am. Chem. Soc.*, 2009, **131**, 15976.
14 Q. W. Jiang, G. R. Li and X. P. Gao, *Chem. Commun.*, 2009, 6720.
15 T. N. Murakami and M. Grätzel, *Inorg. Chim. Acta*, 2008, **361**, 572.
16 G. R. Li, F. Wang, Q. W. Jiang, X. P. Gao and P. W. Shen, *Angew. Chem., Int. Ed.*, 2010, **49**, 3653.
17 K. S. Lee, H. K. Lee, D. H. Wang, N.-G. Park, J. Y. Lee, O. O. Park and J. H. Park, *Chem. Commun.*, 2010, **46**, 4505.
18 D.-H. Kim, J.-H. Heo, D.-J. Kwak and Y.-M. Sung, *J. Electr. Eng. Technol.*, 2010, **5**, 146.
19 G. Veerappan, K. Bojan and S.-W. Rhee, *ACS Appl. Mater. Interfaces*, 2011, **3**, 857.
20 J. K. Chen, K. X. Li, Y. H. Luo, X. Z. Guo, D. M. Li, M. H. Deng, S. Q. Huang and Q. B. Meng, *Carbon*, 2009, **47**, 2704.
21 J. Z. Chen, B. Li, J. F. Zheng, J. H. Zhao, H. W. Jing and Z. P. Zhu, *Electrochim. Acta*, 2011, **56**, 4624.
22 M. X. Wu, X. Lin, A. Hagfeldt and T. L. Ma, *Chem. Commun.*, 2011, **47**, 4535.
23 C. Giordano, C. Erpen, W. Yao, B. Milke and M. Antonietti, *Chem. Mater.*, 2009, **21**, 5136.
24 T. L. Ma, X. M. Fang, M. Akiyama, K. Inoue, H. Noma and E. Abe, *J. Electroanal. Chem.*, 2004, **574**, 77.
25 X. M. Fang, T. L. Ma, G. Q. Guan, M. Akiyama and E. Abe, *J. Photochem. Photobiol., A*, 2004, **164**, 179.
26 X. M. Fang, T. L. Ma, M. Akiyama, G. Guan, S. Tsunematsu and E. Abe, *Thin Solid Films*, 2005, **472**, 242.
27 P. J. Li, J. H. Wu, J. M. Lin, M. L. Huang, Y. F. Huang and Q. H. Li, *Sol. Energy*, 2009, **83**, 845.